From TOD to maps: data processing and map production

Davide Maino

Università degli Studi di Milano, Dip. di Fisica

Observing the Universe with the CMB
22 - 26 April 2014, L'Aquila

Outline

Planck-LFI 30 GHz

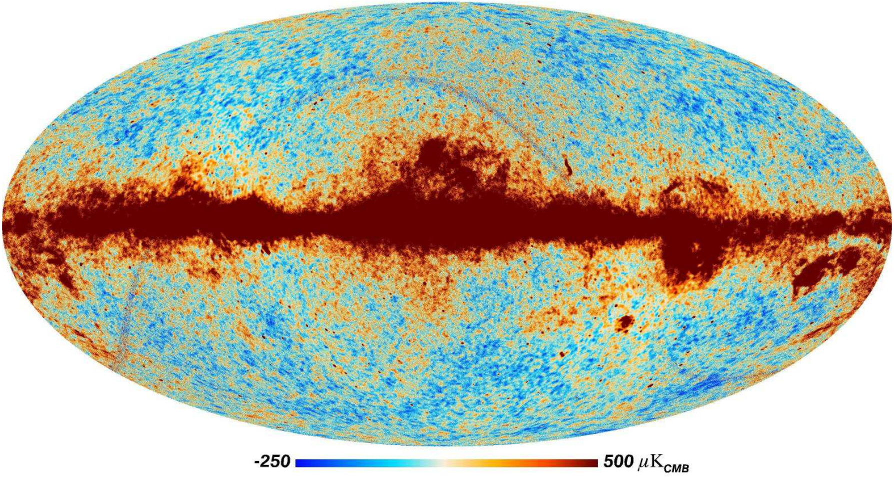

Planck-LFI 44 GHz

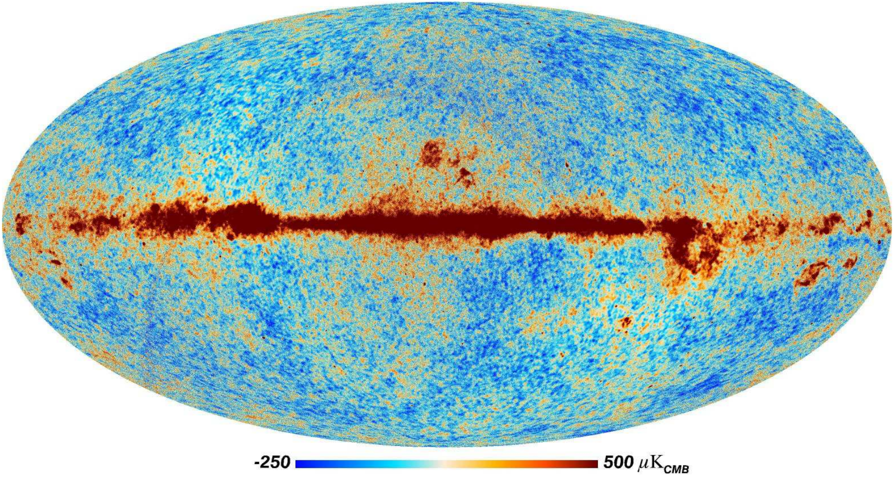

Planck-LFI 70 GHz

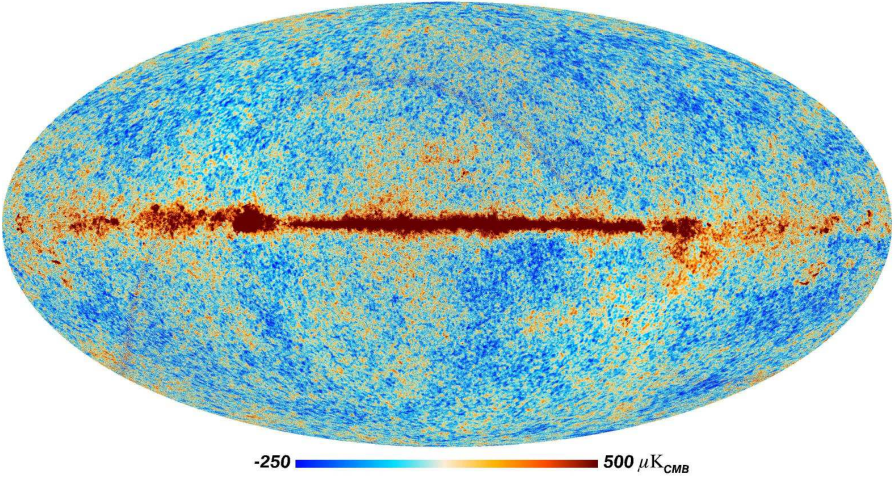

Planck-HFI 100 GHz

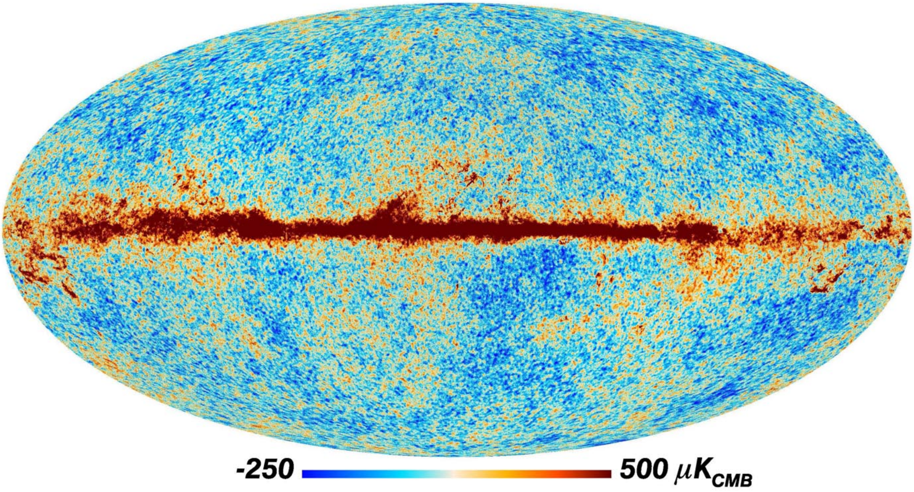

Planck-HFI 143 GHz

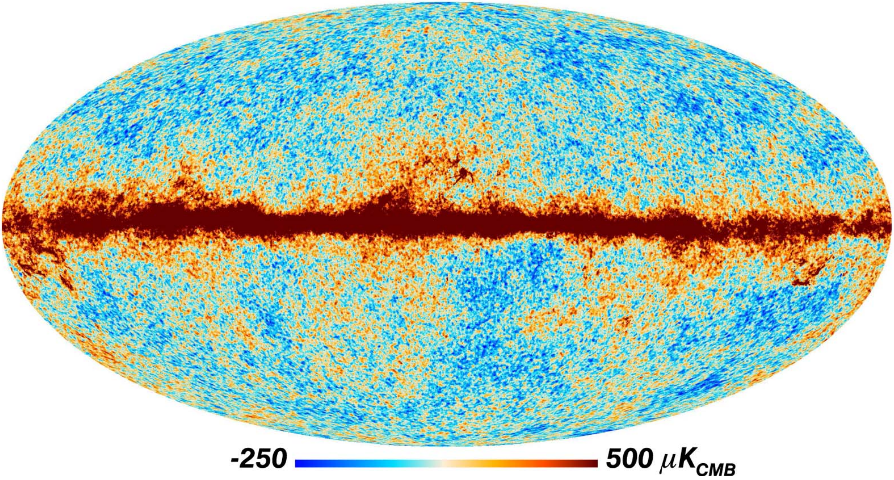

Planck-HFI 217 GHz

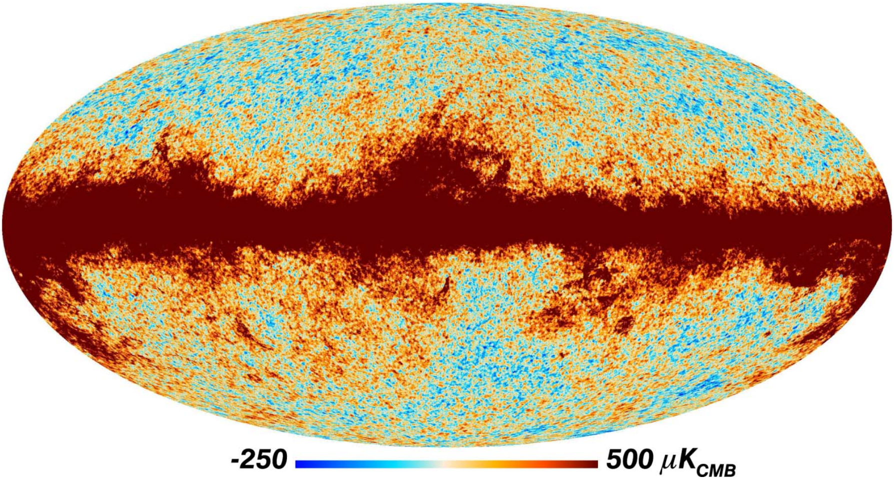

Planck-HFI 353 GHz

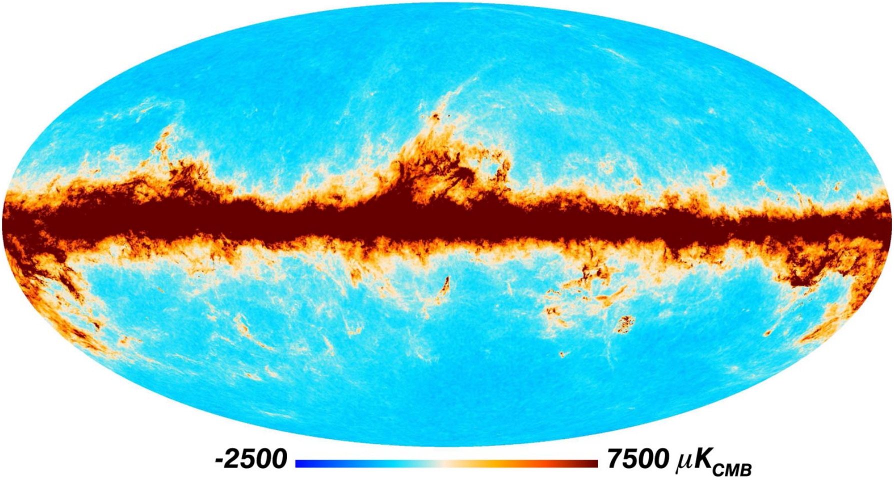

Planck-HFI 545 GHz

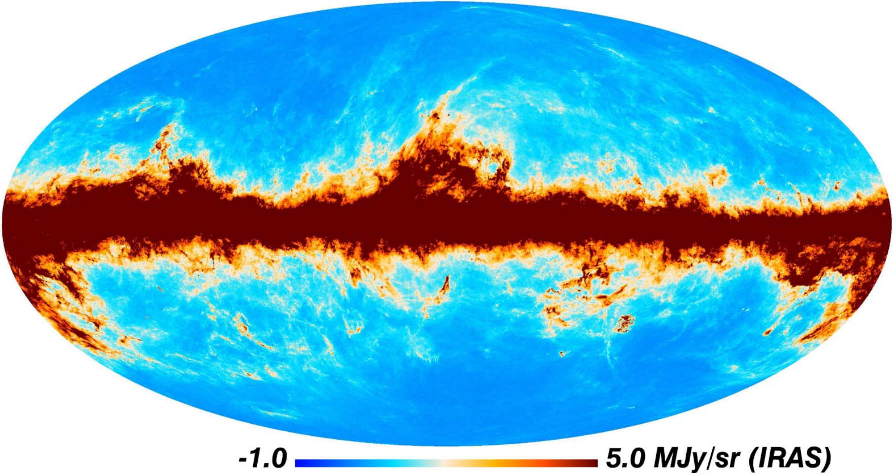

Planck-HFI 857 GHz

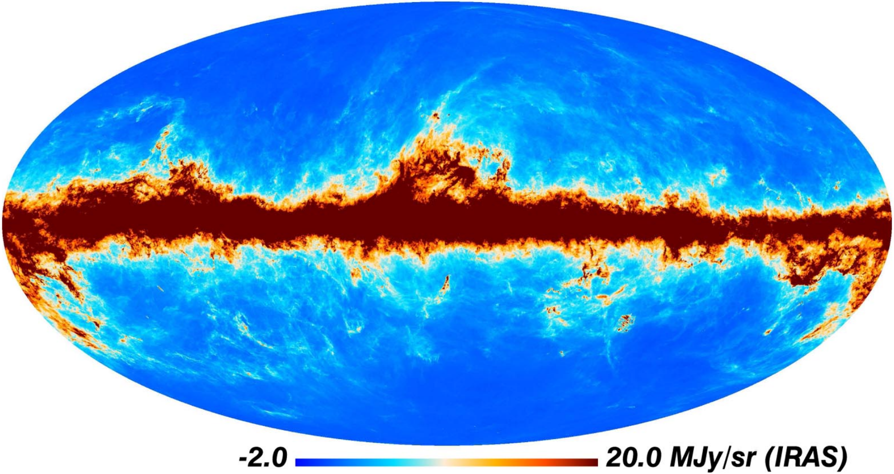

Operations

- *Planck* was launched on 14 May 2009 and the current data release includes temperature maps based on the first 15.5 months of observations
- *Planck* has now ended its operations
  - HFI was switched off on January 2012, beyond the *nominal* period and after supported LFI providing essential H/K telemetry (e.g. 4K cooler)
  - *Planck* was de-orbited on beginning of October and ends its life on 23$^{\mathrm{rd}}$ of October 2013
- Data are of incredible quality!

Data Processing Overview

- Both DPCs (LFI and HFI) approach data reduction with specific tasks aiming to estimate and correct instrumental systematic effects
- There are three main logical levels:
  - Level 1: H/K and Science telemetry from the satellite are transformed into raw timelines and stored into dedicated databases with the associated time information
  - Level 2: instrument information is gathered and ingested into the Instrument Model, removal of systematic effects, flag data of suspected quality, photometric calibration and creation of maps and ancillary products
  - Level 3: more science here with component separation, power spectra estimation and extraction of cosmological parameters
- Each step is internally validated (with dedicated sims) and most of the DPC work is spent cross-checking internally and between the two instruments (which adds a strong value to validation)

From raw data to maps

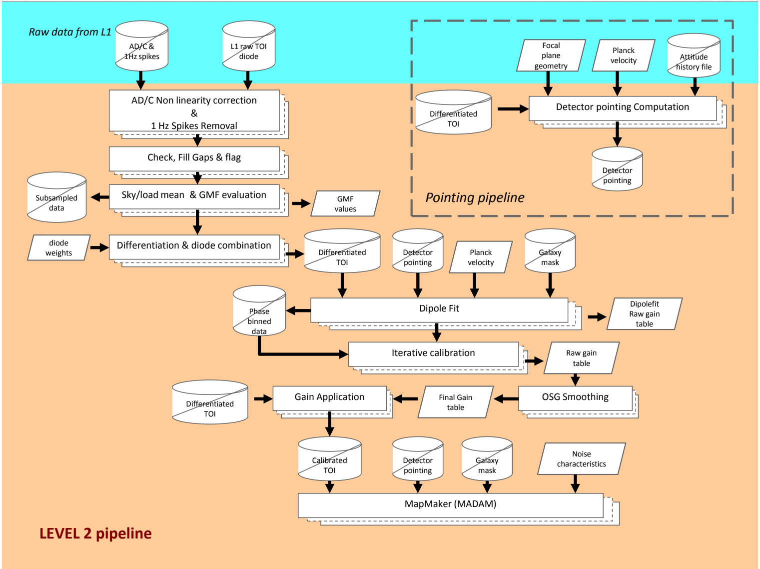

Data Flagging

- During L1 and L2 pipelines, data are checked sample-by-sample and un-usable samples (manoeuvres, special operations) are properly flagged
- LFI: about 1% of data are flagged due to instrument anomaly
- HFI: most of flagged data are due glitches and special processing/flagging has been developed

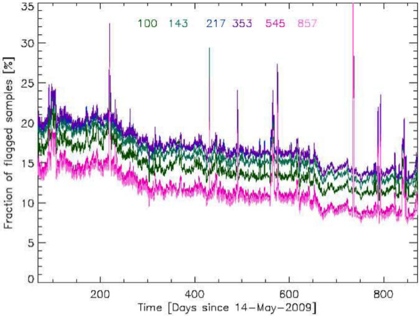

Beams reconstruction

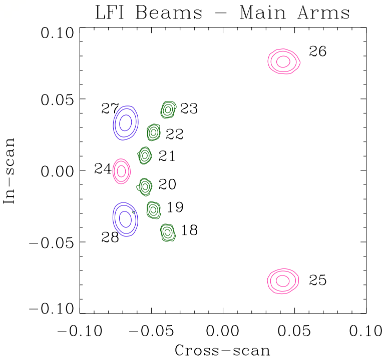

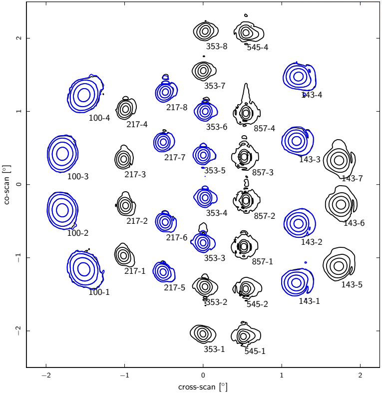

- Beams contours (-20dB/LFI or -30dB/HFI) from planet transits (Jupiter/Mars)

LFI real beams

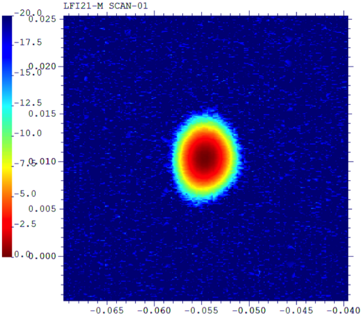

$2', \tau = 3600$sec

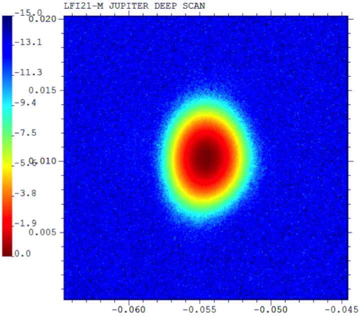

$0.5', \tau = 2900$ sec

Pointing Reconstruction

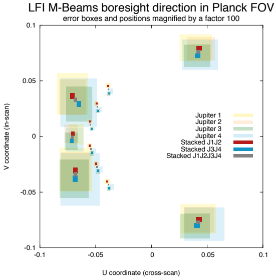

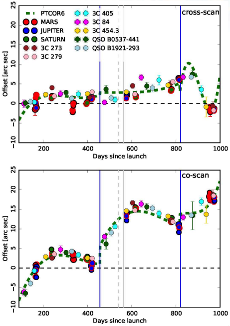

- Pointing reconstruction has an error of $0.2'$ with several corrections applied due to stellar aberration and wobble angle (thermo-elastic deformation)
- LFI: only one discontinuity (switch-over of sorption-cooler)
- HFI: PTCOR model (now used by LFI too) combining all data transits and S/C modelling

Wobble Correction

- Making SS1 and SS2 difference show how good pointing reconstruction is
- Especially @30GHz where beams are not symmetric → you expect a butterfly image

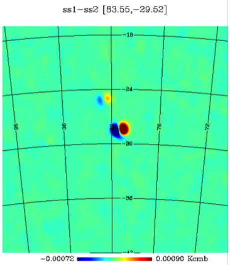

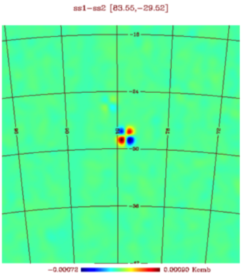

Effective Beams

Band	FWHM [′]	e	Ω [arcmin^2]
70	13.252±0.033	1.223±0.026	200.7±1.0
100	9.651±0.014	1.186±0.023	105.8±0.3
143	7.248±0.015	1.036±0.009	59.9±0.2
217	4.990±0.025	1.177±0.030	28.5±0.3

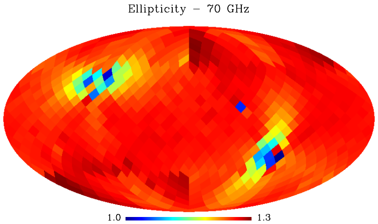

- Scanning beams are used to compute effective beams which gives pixel-by-pixel the beam shape projected in the sky when scanning strategy is accounted for. Fundamental point for source extractions and beam window function

Photometric Calibration - 0

- This is the most important and critical aspect of data reduction.
- Need a well known calibration source, always visible during observations and with same spectral shape of the signal one wants to measure
- CMB Dipole due to Sun motion wrt CMB rest frame is such a source - at least for frequency where CMB signal is strong
- Do a simple χ^2 fit

$$\chi^2 = \sum_{i \in k} \frac{\left[\Delta V(t_i) - g_k \left(D_S(t_i) + D_P(t_i)\right) - b_k\right]^2}{\sigma_i^2}$$

where sum is extended to all valid samples within the k pointing period, D_S and D_P are expected dipoles signal due to Sun and *Planck* motions respectively and g_k and b_k are gain and baseline for the k pointing period.

Photometric Calibration - I

- The LFI calibration pipeline works as follows
  - estimate dipole amplitude and alignment of dipole for any direction
  - create the expected level of the dipole signal accounting for the full-beam shape
  - fit real data with dipole with iterative approach (raw gains)

$$\begin{tikzcd} \text{calibration} \arrow[r] & \text{making map} \arrow[r] & \text{improve sky model} \arrow[ll, bend right] \end{tikzcd}$$

  - filter raw gains or use 4K H/K information to calibrate data

Photometric Calibration - II

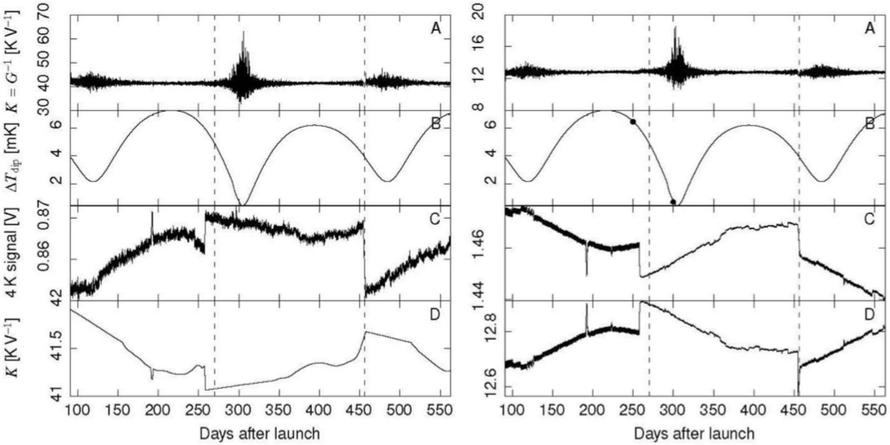

30 GHz 70 GHz

Photometric Calibration - II

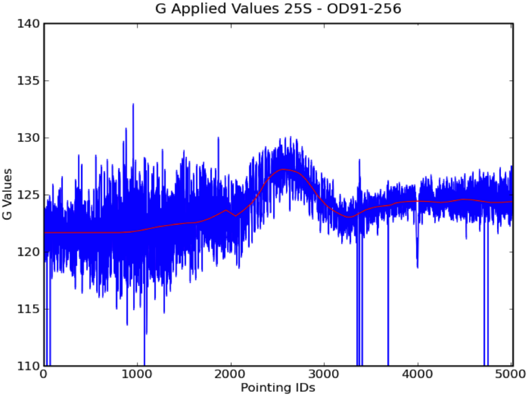

Photometric Calibration - II

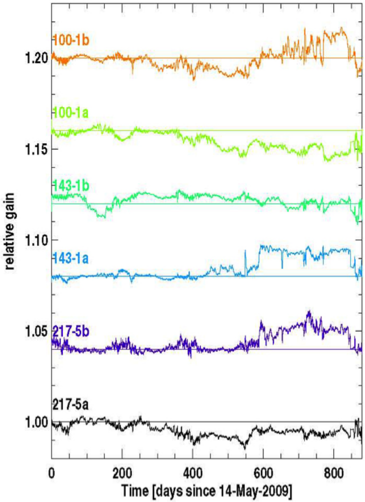

Map-making - I

- From calibrated timelines we have to construct maps
- Let us assume:

$$d_t = P_{ti}\Theta_i + n_t$$

where i is the pixel index, d_t is the data stream ordered in t, n_t is the instrument noise and P_{ti} is the pointing matrix

- Noise has to be known at least its statistical properties

$$\langle n_t n_{t'} \rangle = \mathcal{N}_{tt'}$$

- Θ_i is extracted from data (inversion)
- Maps are $10^6 \div 10^7$ pixels and inversion costs N^3_{pixels} operations

Map-making - II

- Which is the best way to create a map from TOD?

$$\chi^2 = \sum_{tt'ij} (d_t - P_{ti}\Theta_i)\mathcal{N}^{-1}_{tt'}(d_{t'} - P_{t'j}\Theta_j)$$

- Minimize with respect to Θ

$$\frac{\partial \chi^2}{\partial \Theta_i} = -2 \sum_{tt'j} P_{ti}\mathcal{N}^{-1}_{tt'}(d_{t'} - P_{t'j}\Theta_j)$$

- Solution is

$$\sum_{tt'j} P_{ti}\mathcal{N}^{-1}_{tt'}P_{t'j}\Theta_j = \sum_{tt'j} P_{tj}\mathcal{N}^{-1}_{tt'}d_{t'}$$

$$\Delta_i = \left(P^T \mathcal{N} P\right)^{-1} P\mathcal{N}^{-1}d$$

Map-making - III

- Rewrite Δ with our data model

$$\begin{aligned}\Delta &= \left(P^T\mathcal{N}^{-1}P\right)^{-1}P^T\mathcal{N}^{-1}(P\Theta + n)\\ &= \Theta - \left(P^T\mathcal{N}^{-1}P\right)^{-1}P^T\mathcal{N}^{-1}n\end{aligned}$$

- if $\langle n\rangle = 0$ then $\langle\Delta\rangle = \Theta \rightarrow$ un-biased
- Compute variance

$$\begin{aligned}\mathbf{C}_N &= \langle(\Theta - \Delta)(\Theta^T - \Delta^T)\rangle\\ &= \left(P^T\mathcal{N}^{-1}P\right)^{-1}\end{aligned}$$

Map-making - IV

- Write the problem in terms of the likelihood function

$$\mathcal{L} \propto \exp\left\{-\frac{1}{2}(d_t - P_{ti}\Theta_i)\mathcal{N}^{-1}_{tt'}\left(d_{t'} - P_{t'j}\Theta_j\right)\right\}$$

  and the ML solution is obtained maximising $\mathcal{L}$ e.g. minimising the exponential $\rightarrow \chi^2$

- Theorem:Cramer-Rao Inequality. No estimator can measure Θ_i with error smaller than the diagonal elements of $\mathbf{F}^{-1}$ where $\mathbf{F}$ is the Fisher (or curvature) matrix

$$\mathbf{F}_{ij} = -\frac{\partial^2 \ln\mathcal{L}}{\partial\Theta_i \partial\Theta_j}$$

- Computing this quantity we found that $\mathbf{F} = \mathbf{C}_N^{-1}$ i.e. our estimator is both un-baised and minimum variance

Map-making - V

Destriping

- The non-white component of the noise ($1/f$ noise) is well approximated by a baseline for each scan circle

$$d_t = P_{ti}\Theta_i + n_{t,corr} + n_t = P_{ti}\Theta_i + F_{tj}a_j + n_t$$

where F_{tj} is 1 if point t lies on scan circle j

- We can solve the problem in a ML fashion

$$\Delta = \left(P^T \mathcal{C}_N^{-1} P\right)^{-1} P^T \mathcal{C}_N^{-1} (d - Fa)$$

- Code solve for baselines a that are subtracted from the original TOD

Map-making - VI

LFI

- Calibrated TOI for each radiometer are input of `madam` map-making code, together with pointing data
- The algorithm is a maximum-likelihood destriping

HFI

- Single rings are projected into sky HEALPix rings and maps for each ring is created by filtering and baseline-subtraction
- These ring maps are used for photometric calibration of each detector
- Calibrated rings are combined via a least-sqaures destriping algorithm

Maps production

- Maps produced at different levels:
  - Single Radiometer/detector maps
  - Frequency maps (optimally combining TOD from each radiometer/detector)
  - Half-Ring (HR) maps: created from the first and second part of each pointing period
  - Survey and Years maps: created from data spanning single surveys/years observing periods
  - Low resolution maps used for the computation of the noise covariance matrix

Systematic effects

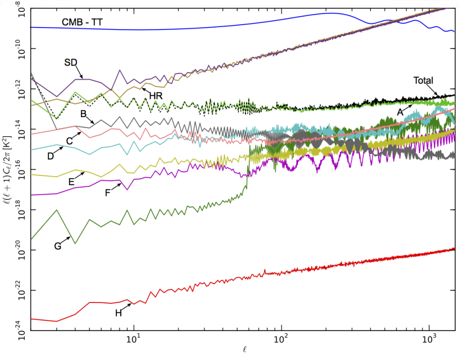

- Null tests: primary tool to see systematic effect residual w.r.t. white noise level
- Sims: Assess their impact on TOI using in-flight H/K data. This approach provides a powerful tool to check for systematics

44 GHz

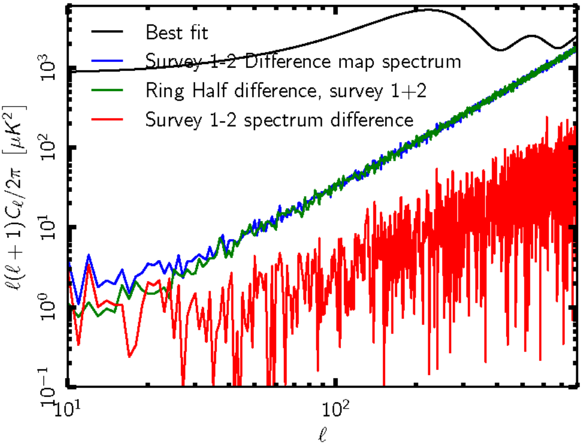

Best fit
Survey 1-2 Difference map spectrum
Ring Half difference, survey 1+2
Survey 1-2 spectrum difference
$\ell(\ell+1)C_\ell/2\pi\ [\mu K^2]$
10^{-1}
10^{0}
10^{1}
10^{2}
10^{3}
10^{1}
10^{2}
ℓ

70 GHz

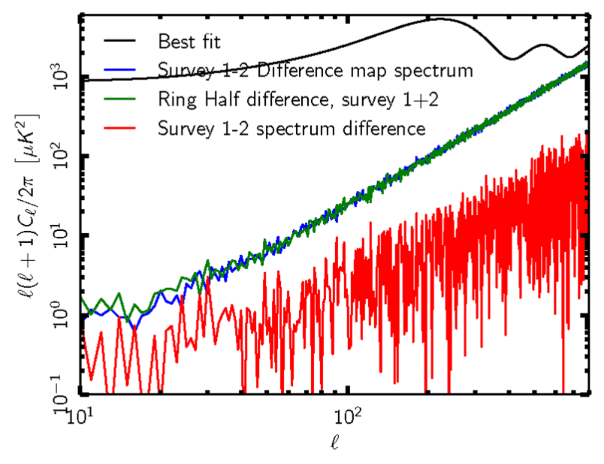

Best fit
Survey 1-2 Difference map spectrum
Ring Half difference, survey 1+2
Survey 1-2 spectrum difference
$\ell(\ell+1)C_\ell/2\pi\ [\mu K^2]$
10^{-1}
10^0
10^1
10^2
10^3
10^1
10^2
ℓ

LFI Internal Validation - Null tests

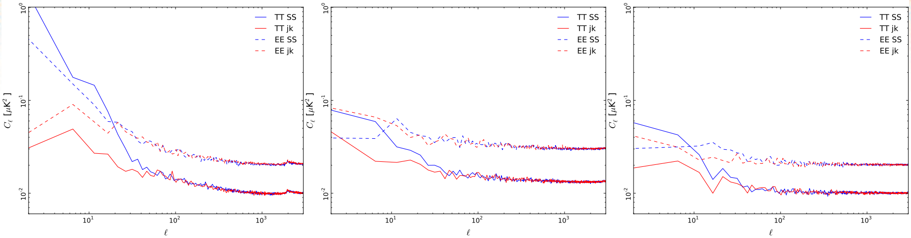

- Quality of LFI maps is assessed and verified by a set of null-tests in an almost automatic way
- Several data combination (radiometer, horn-pairs, frequency) on different time-scales (1 hour, survey, full-mission): difference at horn level at even/odd surveys clearly reveals side lobe effect
- Null-test power spectra are used to check total level of system. effects to be compared w.r.t. white noise level and systematic effects analysis

LFI Internal Validation - Check Spectra

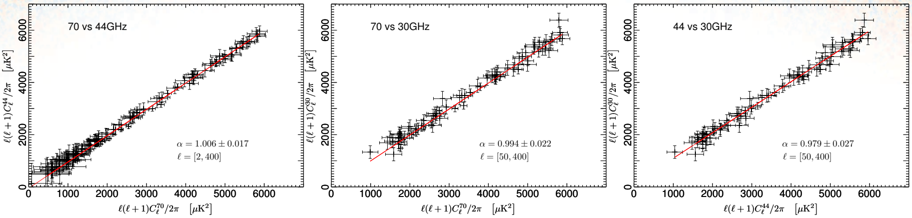

- Compute power spectra in multipole range around the first acoustic peak removing the unresolved point source contributions. Spectra are consistent within errors. 30 and 44/70 have different approaches to gain applied
- Hausman test assess consistency at 70 GHz showing no statistically significant problem
- Spectra from horn-pairs and from all 12 radiometers: χ^2 analysis shows compatibility with null-hypothesis

Inter-Instrument Validation - I

- Consistency between LFI and HFI performed comparing frequency maps from 44 to 217 GHz
- Crucial is the comparison between 70 and 100 GHz where CMB is dominating

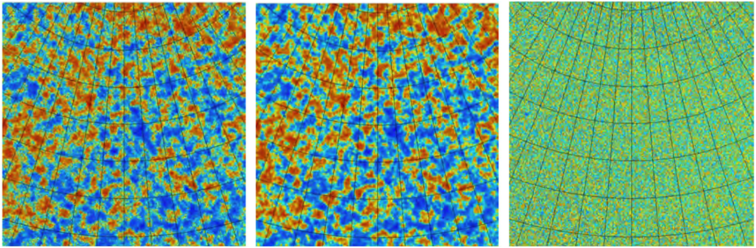

70GHz 100 GHz Difference

Inter-Instrument Validation - II

- Check effects of possible inter-calibration mismatch
- Use SMICA (CMB component separation method - see Delabrouille's talk today) from 44 to 353 GHz and using 143 as reference
- HFI maps are consistent at 0.2% level and consistency between 70 and 100 is at the 0.3% level

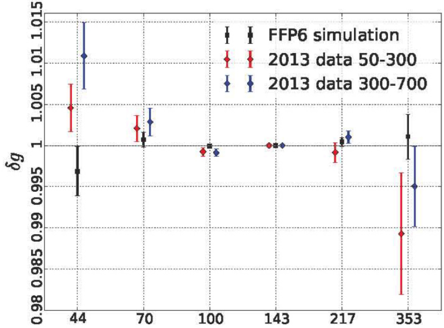

Maps Characteristics

Uncertainty	Applies to	Method
Gain calib	All sky	*WMAP* dipole
Zero level	All sky	Galactic Cosecant model
Beam	All sky	GRASP models via FeBecop
CC	non-CMB	ground/flight bandpass leakage
Resid. Sys	All sky	Null-tests

Property	30	44	70
Frequency [GHz]	28.4	44.1	70.4
Noise rms/pixel [μK_{CMB}]	9.2	12.5	23.2
Gain Uncert	0.82%	0.55%	0.62%
Zero Level Uncert [μK_{CMB}]	±2.23	±0.78	±0.64

What's next?

- Polarisation data will open new possibilities: direct measure of τ, new hints on tensor modes, break some parameter degeneracies with temperature only data
- Foregrounds polarisation maps will provides informations on, e.g., emission mechanisms and structure of galactic magnetic field
- Challenging due to the tiny CMB polarisation signal but ...

What's next?

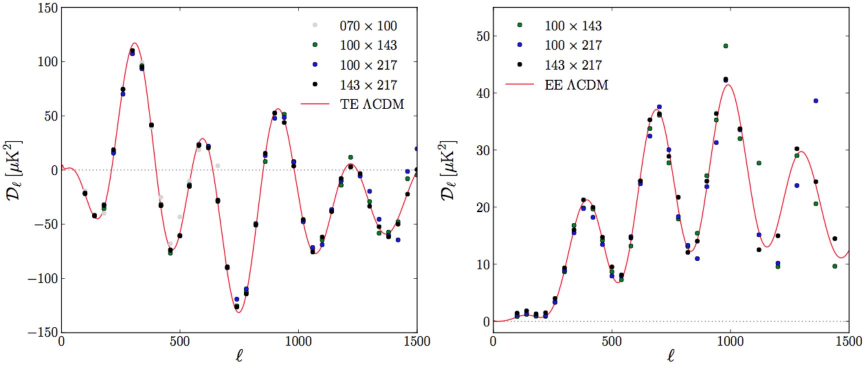

- Angular power spectra of TE (left) and EE (right) from *Planck* data combinations. $f_{sky} = 0.4$, no foreground cleaning, uniform weight of channels